ORIGINAL PAPER

Ground Motion Parameters and Resonance Effect During Strong Earthquake in Northern Thailand

Lindung Zalbuin Mase · Suched Likitlersuang · Tetsuo Tobita

Abstract Several previous investigations have suggested that ground motion as described by various parameters and resonance effects could have contributed to the damage observed during an earthquake. This paper presents a ground motion parameters study and site investigation in Northern Thailand during the Tarlay Earthquake of 2011. Ground motion parameters recorded at the closest seismic station to the earthquake rupture, i.e. Mae Sai Station (MSAA) are studied. Microtremor measurement was performed at the MSAA site. The horizontal to vertical spectral ratio (H/V) from the investigation are interpreted. Spectral acceleration ratios based on data from the MSAA are compared to determine the possibility of resonance during the earthquake. Spectral acceleration data based on recorded ground motion are compared to guideline design spectral acceleration to determine the critical period. Results show that during the Tarlay Earthquake, significant duration was 24 s. Within this duration, resonance was plausible within the frequency range of 1.82 to 2.1 The critical period ranged from 0.4 to 0.6 s, indicating that low-medium story buildings were most vulnerable. Results also show that horizontal ground motion was relatively dominant in the destruction of structural buildings during the earthquake.

Keywords Ground motion · Microtremor · Resonance · Northern Thailand · Tarlay Earthquake

L. Z. Mase
Department of Civil Engineering, Faculty of Engineering, University of Bengkulu, Bengkulu 38371, Indonesia
e-mail: lmase@unib.ac.id

S. Likitlersuang (✉)
Department of Civil Engineering, Centre of Excellence in Geotechnical and Geoenviromental Engineering, Faculty of Engineering, Chulalongkorn University, Bangkok, Thailand
e-mail: fceslk@eng.chula.ac.th

T. Tobita
Department of Civil, Environmental, and Applied System Engineering, Kansai University, Osaka, Japan
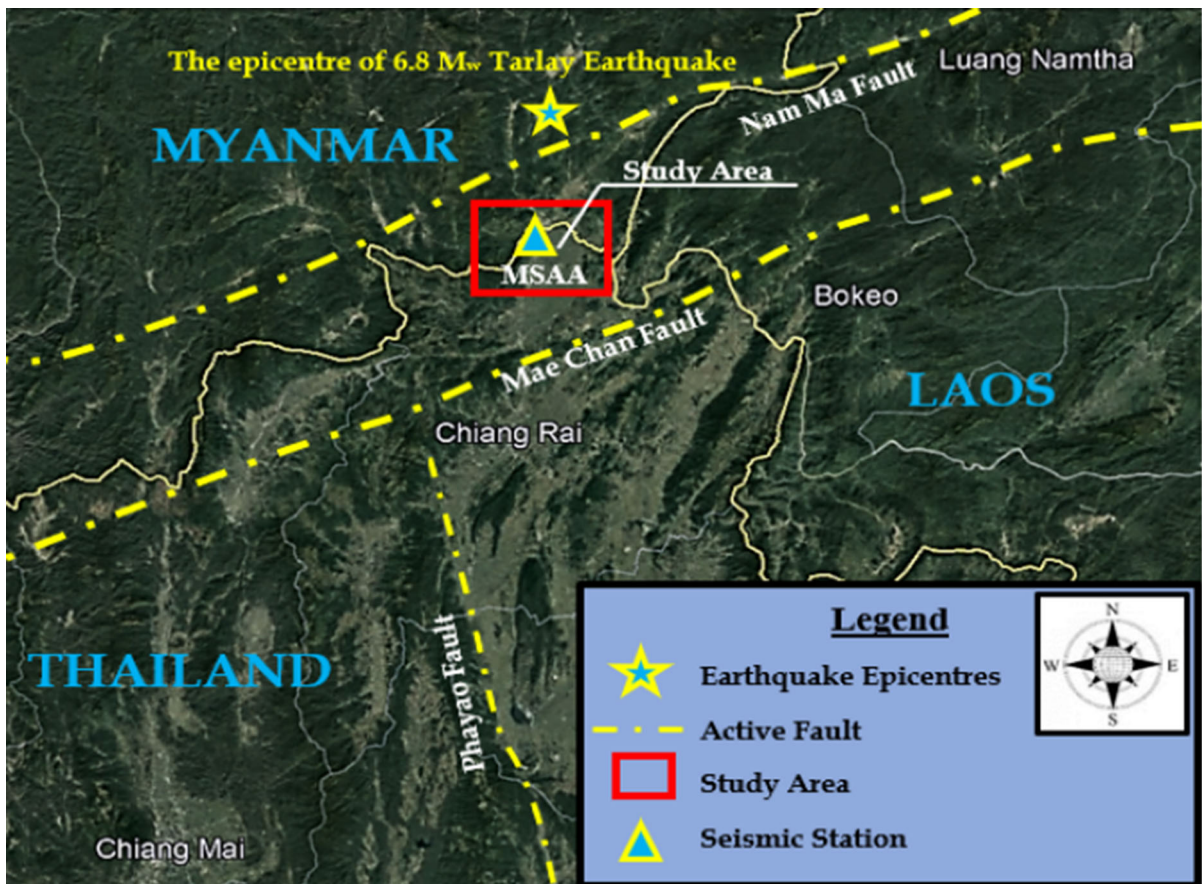e-mail: tobita@kansai-u.ac.jp

1 Introduction

Chiang Rai Province is a well-known trade and tourist zone in Northern Thailand which experienced an economic boom in the 1980s. Unfortunately, earthquake threats have become a pressing issue in this area. A recent significant earthquake that took place in Northern Thailand on March 24, 2011 was the 6.8 M_w Tarlay Earthquake positioned near the Thailand-Myanmar border. This earthquake resulted in very serious damage, especially in Mae Sai District, Chiang Rai Province, Northern Thailand (Fig. 1), 33 km from the earthquake's epicentre. The hypocentre was located at 20.705 N, 99.949E with the focal depth of

Fig. 1 Area of study, epicentre of Tarlay Earthquake, and surrounding active faults. Modified from Google Earth (2016)

10 km below ground surface (Phodee et al. 2015). Mae Sai District is also the most northern district in Thailand and a gateway between Thailand and Myanmar. The Tarlay earthquake affected general activities in several neighbouring countries, including Myanmar and Laos PDR (People's Democratic Republic). In addition, Likitlersuang et al. (2020) reported that the Tarlay Earthquake shaking was also felt by people staying in Bangkok, the capital city of Thailand, which is located about 1000 km from the epicenter.

The Thai Meteorological Department (2011) and Soralump and Feungaugsorn (2013) reported that a maximum peak ground acceleration (PGA_{max}) of about 0.207 g was recorded during the earthquake at the closest seismic station (Mae Sai Seismic Station or MSAA) to the earthquake epicentre. Moreover, this earthquake triggered a soil damage phenomenon called liquefaction. Soralump and Feungaugsorn

(2013) noted that this was the first case of observable evidence of earthquake-induced liquefaction found in Thailand since 1943. Through site response analysis during the Tarlay Earthquake, Mase et al. (2018a) mentioned that the Thailand–Myanmar border region is very vulnerable to liquefaction. Mase et al. (2018b) also reported that the Tarlay Earthquake triggered liquefaction at the border of Thailand–Myanmar because of the existence of loose sand layers shallow depth. Meanwhile, structural damage during the Tarlay Earthquake was reported by Ruangrassamee et al. (2012), with the damage dominantly observed on low to medium stories buildings in the vicinity. Similar studies in other areas, such as Flores et al. (1987) and Fischer and Fischer (1998) also reported that the damage could be worse due to the interaction between site effect and propagated wave during the Mexico Earthquake and Northridge Earthquake. This phenomenon is also known as resonance effect. In line

with the fact finding found during the Tarlay Earthquake, it is worth to know the detail how the characteristics of sites and ground motion is. This research goes on to suggest that the damage found during the earthquake might have been caused by the resonance effect between the site and propagated waves, a phenomenon well-known for its contribution to structural and soil damage in several other areas previously hit by earthquakes.

Several intensive studies related to earthquake characteristic and liquefaction identification are also performed by several local researchers. The studies by Ruangrassamee et al. (2012), Mase et al. (2017, 2018a, b) and had presented the general impacts of the Tarlay Earthquake, focusing on reports of structural damage and liquefaction potential estimated by empirical approaches (Seed and Idriss 1971; Youd and Idriss 2001; Idriss and Boulanger 2006). Mase et al. (2020a) performed a verification of liquefaction potential during the Tarlay Earthquake at the border of Thailand–Myanmar and found that several sites could be potentially experiencing liquefaction at shallow depth. Tanapalungkorn et al. (2020) conducted a statistical analysis to observe the characteristic of earthquake ground motion in Northern Thailand, including the Tarlay Earthquake and suggested NGA-West2 are the most appropriate attenuation models to predict ground motion in Northern Thailand. However, what these previous studies lack are detailed specific description of the local site conditions, and ground motion parameters alongside verification of resonance effects during the Tarlay Earthquake.

This study presents the ground motion parameters and local site observations during the Tarlay Earthquake based on microtremor measurements taken at the closest seismic station to the rupture (Fig. 1). Interpretations of ground motions, such as peak ground motion amplitude, duration, and energy content are presented. The earthquake's predominant frequency (f_0) and amplification ratio (horizontal to vertical spectral ratio or H/V ratio) are also presented. The study then compares the spectral ratio between measured H/V with recorded ground motion for resonance prediction. A comparison of this study's results to the guideline design spectral acceleration stipulated in the Seismic Design Code of Thailand is presented at the conclusion of this study. In general, the results from this study would give a better understanding of resonance effects during strong earthquakes in Northern Thailand, and provide recommendations to prepare against earthquake impacts in the region.

2 Geological Condition Study Area

The geological map of the area under study is presented in Fig. 2. There are generally three dominant geological formations in the Mae Sai Basin, Northern Thailand. The first one is a fluvial deposit (Qff), which is composed of sediments and coarse materials such as sands, gravels, silts, and clay materials. MSAA seismic station (M-1), and Borehole-2 (BH-2) where core sampling was taken to characterise the Mae Sai Basin, are both located on this fluvial deposit formation. The other two geological formations are a chert deposit (CPk), made up of sandstone, limestone, and shale, and basic igneous rock (PTrv). These formations are generally found in Thailand's mountainous areas which were formed during the Permian to the Carboniferous ages (Thai Department of Mineral Resources or TDMR 2017).

Geological condition of Northern Thailand had been presented by previous studies, such as Thay et al. (2013), Mase et al. (2018a, b, 2020a, b). Generally, sand layers followed by thin clay layer are found in Northern Thailand. In line with these previous studies, Fig. 3 presents the geological condition of the Mae Sai Basin. Site investigations at BH-2 have determined that the Mae Sai Basin is dominated by sandy soils. Ground water is found at a depth of 1.2 m. At shallow depth, loose sandy soils classified as SP-SM with average The corrected value of standard penetration test or $N_{1(60)}$ about 8 blows/ft and fines content (FC) of 18% are found up to 9 m depth, then followed by silty sands (SM) with average $N_{1(60)}$) about 10 blows/ft, FC = 18% from 9 to 16.5 m. Mixed-gravelly-sandy soils (SM-GM and GP) with average $N_{1(60)} \sim 15$ blows/ft, FC = 19% lie at 16.5–19 m and Clayey sand (SC) layers with average $N_{1(60)} \sim 15$ blows/ft, FC = 20% lie at 19–20.5 m. SM and SC layers are again found at 20.5–23.5 m and 23.5–30 m of depth, respectively. The "time averaged shear wave velocity for the first 30 m of depth" (V_{s30}) at BH-2 was about 200 m/s; this makes the basin "Site Class D" based on the National Earthquake Hazard Reduction Program (NEHRP 1998). Of note are the saturated sand layers
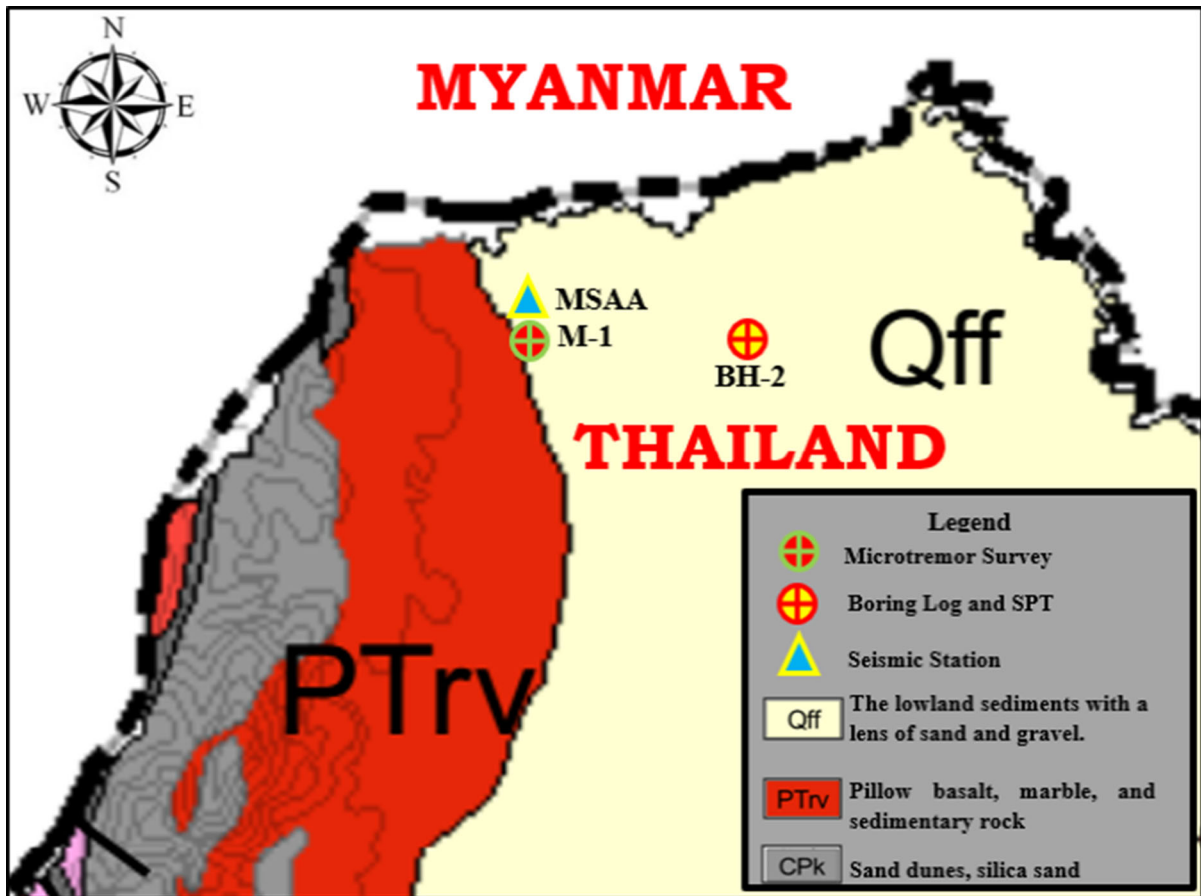
Fig. 2 The geologic map and observed points

at shallow depth, which, as Mase et al. (2018b) reported, were liquefied during the Tarlay Earthquake near the Thailand–Myanmar border.

3 Theory and Method

3.1 Ambient Noise Measurement Using Microtremor

Lachet and Bard (1994) previously stated that geophysical measurements obtained with microtremor equipment can provide insight for application in seismic ground response between sediment and bedrock. The observation of local site using microtremor was introduced by Kanai and Tanaka (1954). Both Lachet et al. (1996), Bard (2004), El-Hady et al. (2012), Mase et al. (2020b) have utilised microtremor measurements to characterise site conditions; the most

popular method of characterisation is to compare horizontal to vertical spectral accelerations, also known as an H/V ratio. The empirical correlation to calculate H/V ratio from microtremor measurement is based on the work of Nakamura (1989). H/V is the horizontal to vertical spectral ratio derived from the fast Fourier's Transform (FFT) of the ambient noise from microtremor measurements. This parameter is generated from the transfer function of ground motion, which is also capable of predicting the predominant period (T_0) and amplification of peak H/V. It is also able to estimate sediment thickness probabilities and be used to describe the impedance contrast. Atakan (2009) has found that there is a consistency between H/V yielded from microtremor measurements and H/V recorded during an earthquake.

In this study, the result of microtremor measurements, or seismographs, are further analysed using the Fast Fourier Transform Method to obtain H/V.
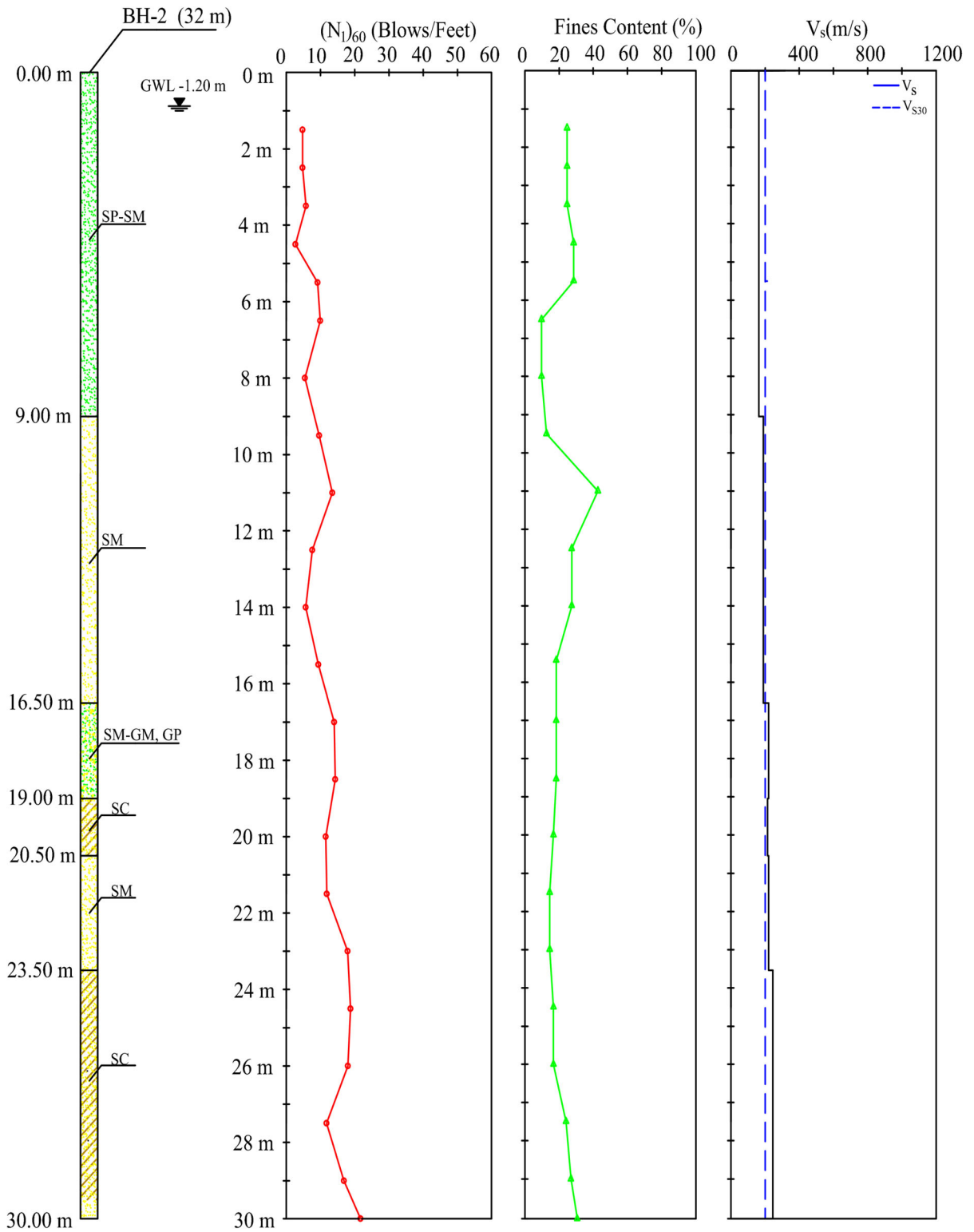
Fig. 3 Typical subsoil condition of Mae Sai Basin

Microtremor and earthquake H/V values are then compared to each other, corresponding to frequency. A site's H/V ratio is estimated based on comparing the shear wave (V_s) on the vertical and horizontal directions, as expressed by the equation:

$$H/V = \sqrt{\frac{H_{(EW)}^2 + H_{(NS)}^2}{2V^2}} \qquad (1)$$

where $H_{(EW)}$ and $H_{(NS)}$ are the horizontal spectral values in the east–west (EW) and north–south (NS) directions, respectively, and V is the vertical spectral value.

In general, H/V is relatively more stable than raw noise spectra, as confirmed by the works of Lachet et al. (1996) and Koçkar and Akgün (2012). Several researchers have stated that H/V is normally interpreted with the predominant frequency, or f_0. However, this interpretation is still debated and frequently reviewed, especially when related to determining the H/V. This is due to the fact that noise caused by human factors and environmental settings could influence the quality of measurements. Other factors, such as Poisson's ratio (ν) and receiver restriction are also capable of affecting the reliability of H/V (Bonnefoy-Claudet et al. 2006). Due to these nature and human influences, H/V is then not overall clarified. Despite these complications and limitations of the reliability of a local site's H/V values, Raptakis et al. (2005) states that there is a common perception where f_0 values obtained from microtremor measurements are reliable.

Ambient noise was measured with a seismometer, model DATAMARK JU410, equipped with a 24-bit digital acquisition device, fabricated by Hakusan Co.Ltd. This microtremor equipment has 3 accelerometers component, i.e. north–south (NS), east west (EW), and up–down (UD), that were used to observe the strong and weak motions on the investigated site (2008). The microtremor equipment tends to have lower sensitivity than compared with the seismometer sensors (Bard 2004; Koçkar and Akgün 2012). The JU410 model is relatively more sensitive to detecting ambient noise and vibration that are used to determine spectral ratios than other kinds of accelerometer sensors. In addition, electrical noise during measurements were minute and could be neglected. Signal duration was set at 1000 s, and sampling frequency at 100 Hz, based on the suggestions of Koçkar and Akgün (2012). Digitizers were warmed-up for 5 min

prior to measurements to avoid problems associated with the low frequency range and to ensure the quality of a digitized waveform. After that, measurements of ambient noise were performed for 30 min (Mase et al. 2020b). In this study, the expected minimum frequency from each measurement is about 1 Hz (Koçkar and Akgün 2012).

In line with the investigation to the effect of ground motion to the sites, the resonance effect between the ground and the earthquake is also aimed to measure in this study. Gosar (2010) stated that the resonance effect can be observed by comparing the predominant frequency of the investigated site's and the earthquake's horizontal-to-vertical spectral acceleration ratios, or H/Vs. Equation 2 expresses the relationship between site H/V and earthquake H/V that is used to predict resonance vulnerability:

$$R = \frac{|f_0 Site - f_0 Earthquake|}{f_0 Earthquake} \times 100\% \qquad (2)$$

where R is the resonance vulnerability between site and earthquake motion, and $f_0 Site$ and $f_0 Earthquake$ are the site's and earthquake's predominant frequency, respectively.

3.2 The Importance of Ground Motion Parameters

Bommer and Martínez-Pereira (2000) have stated that ground motion parameters are important for interpreting ground motion characteristics. Misliniyati et al. (2019) also mentioned that the ground motion parameters could be used as one of methods to determine the appropriate soil models in one dimensional seismic ground response analysis. Mase et al. (2018a) assigned the main ground motion parameters as the indicator to determine the suitable attenuation. In line the use of ground motion parameters elaborated in previous studies, it is therefore important to observe ground motion parameters, especially during the strong earthquakes.

The importance of understanding ground motion characteristics lies in identifying potential damage during seismic wave propagation. Kramer (1996) listed three main parameters to describe ground motion characteristics: amplitude parameters of vertical array, frequency content, and shaking duration. Seismosoft (2018) explains that ground motion parameters have to be first identified to obtain the

specific characteristics of ground motion. Seismosoft (2018) also proposed additional ground motion parameters which can help engineers to understand the characteristic of ground motion; these parameters are maximum acceleration (PGA_{max}), maximum velocity (PGV_{max}), maximum displacement (PGD_{max}), time values of PGA_{max}, PGV_{max}, PGD_{max}, the ratio V_{max}/A_{max}, root-mean-square (RMS) values of acceleration, velocity, displacement, Arias intensity, characteristic intensity, specific energy density, intensity of spectrum responses, Housner intensity, effective duration, and energy flux. One of these parameters, the Arias intensity, is usually recorded as the level of acceleration containing up to 95% of detected Arias intensities, or A95. The significance of the Arias intensity was noted by Arias (1970) for its usefulness in predicting the significance of shaking duration from each ground motion. Several of these parameters are analysed in this study as they were recorded by the MSAA station during the Tarlay Earthquake.

4 Results and Discussion

4.1 Ground Motion Parameters of Tarlay Earthquake

The peak ground accelerations on each direction during the Tarlay Earthquake are interpreted in Fig. 4. There are three peak ground acceleration records representing the ground motion on the directions of EW (East–West), NS (North–South), and UD (Vertical). All records show that peak ground acceleration on a defined direction range from 0.114 to 0.207 g, with the largest value coming from the horizontal EW ground motion. According to Mase et al. (2018a), this ground motion falls into the typical range as recorded at rock sites. Other ground motion parameters recorded by the MSAA station which were analysed are presented in Table 1. Parameters such as maximum value, time of maximum value, energy, ground motion intensity, and root mean square (RMS) value are observed. Based on analysis, ground motion along the NS direction has the largest maximum peak ground velocity (PGV_{max}) at 101.299 cm/s. The maximum time of PGV_{max} was equal in all directions at 59.990 s. The largest maximum peak ground displacement (PGD_{max}) is 5.111 m in the NS-direction. The time
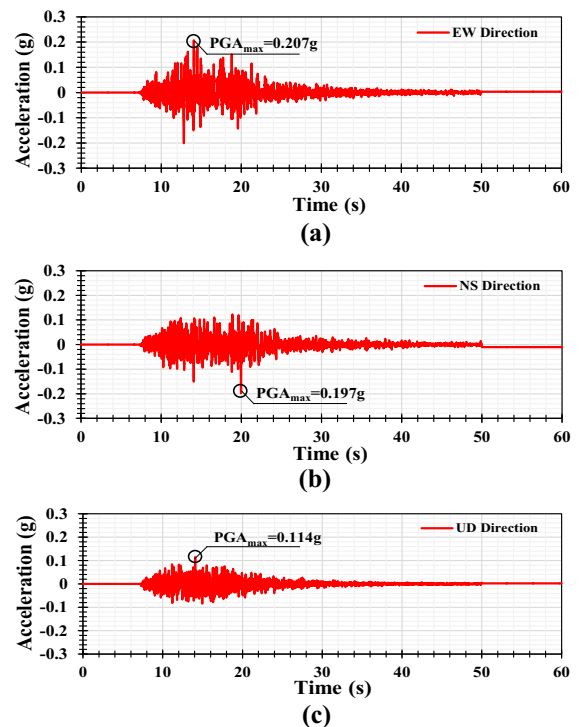

Fig. 4 Ground motion records in: **a** EW direction **b** NS direction **c** UD direction (TMD 2011)

of PGA_{max} during the Tarlay Earthquake ranges from 14.065 to 19.955 s. In regard to energy, the largest recorded specific energy density was in the NS-direction.

The Arias intensity in each direction during the Tarlay Earthquake is presented in Fig. 5, as are the recorded parameters of energy flux and significant duration. As seen in Fig. 5, the Arias intensity in each direction significantly increased at 10 s and continued to climb to a peak at 35 s. Energy flux increases more gradually for the first 52 s in each direction of ground motion, before significantly increasing up to 60 s. For maximum values of energy flux in each ground motion direction ranges from 1800 to 35,000 cm^2/s. A significant duration is defined as the time duration between when 5% of Arias intensity ($t_{5\%}$) and 95% of Arias intensity ($t_{95\%}$) are reached. From Fig. 5, it can be seen that the significant duration of the Tarlay Earthquake ranges from 14 to 21 s. In general, the NS direction had the largest energy flux and significant duration.

Table 1 Analysed ground motion parameters of Tarlay Earthquake recorded at MSAA

| Parameters (unit)	Unit	Motion on EW	Motion on NS	Motion on UD	References
PGA_{max}	g	0.207	0.197	0.114	Kramer (1996)
Time of PGA_{max}	s	14.065	19.955	14.070	Kramer (1996)
PGVmax	cm/s	32.234	101.299	22.969	Kramer (1996)
Time of PGV_{max}	s	59.990	59.990	59.990	Kramer (1996)
Max. displacement	m	1.544	5.111	1.136	Kramer (1996)
PGD_{max}	s	59.990	59.990	59.990	Kramer (1996)
PGV_{max}/PGA_{max}	s	0.159	0.523	0.205	Kramer (1996)
Acceleration RMS	g	0.025	0.024	0.015	Kramer (1996)
Velocity RMS	cm/s	7.826	23.906	5.508	Kramer (1996)
Displacement RMS	m	0.277	0.941	0.206	Kramer (1996)
Arias Intensity	m/s	0.573	0.521	0.207	Park et al. (1985)
Characteristic intensity	Ic	0.030	0.028	0.014	Cabañas and Benito (1997)
Specific energy density	cm^2/s	3674.448	34,282.936	1820.112	Kramer (1996)
Cumulative absolute velocity	cm/s	745.782	809.977	466.346	Cabañas and Benito (1997)
Acceleration spectrum intensity	gsec	0.164	0.129	0.083	Von Thun et al. (1988)
Velocity spectrum intensity	cm	50.280	41.915	21.725	Von Thun et al. (1988)
Housner intensity	m	39.818	36.562	18.972	Kramer (1996)
Sustained maximum acceleration	g	0.183	0.122	0.084	Nuttli (1979)
Sustained maximum velocity	cm/s	10.432	9.120	6.437	Nuttli (1979)
Effective design acceleration	g	0.193	0.189	0.109	Benjamin JR and Associates (1988)
A95 parameter	g	0.202	0.195	0.112	Sarma and Yang (1987)
Predominant period	s	0.140	0.100	0.100	Kramer (1996)
Mean period	s	0.328	0.314	0.228	Rathje et al. (1998)

4.2 Resonance of Tarlay Earthquake and Spectral Acceleration Comparison

Figure 6 presents the comparison of H/V ratios between ground and earthquake motions at M-1. Generally, H/V from the Tarlay Earthquake and from microtremor measurements are consistent and similar with each other, and thus can be compared to one another. From Fig. 6, it can be seen that the predominant frequency (f_0) of ground motion during the Tarlay Earthquake from MSAA was 1.82 Hz, and from M-1 was 2.1 Hz, which are relatively similar. The predominant period (T_0) of the Tarlay Earthquake was 0.46 s, and of the M-1 site was 0.55 s. In other words, resonance effects are plausible within this frequency range. These results also imply that the M-1 site tends to suffer from more impactful shaking during earthquake events since the site vibrates along with wave propagation. Based on the estimation from Eq. 2, the resonance value between the local ground and the Tarlay Earthquake's motions at M-1 is about 15%, which is categorised as a medium-high level of resonance vulnerability.

The Thai Design Seismic–Seismic Design Code of Thailand (2009) outlines design spectral accelerations based on a 2% probability of exceedance or return period of 2475 years, and a 10% probability of exceedance or return period of 475 years. Figure 7 compares both design spectral accelerations outlined in Thai Design Seismic to the spectral accelerations recorded at MSAA during the Tarlay Earthquake in each direction (NS, EW, and Vertical). It can be seen in Fig. 7 that a maximum spectral acceleration of 0.72 g was recorded during the Tarlay Earthquake, which exceeds the design spectral acceleration based on 10% probability of exceedance. This maximum

Fig. 5 Ground motion records in: **a** EW direction **b** NS direction **c** UD direction

(a)

(b)

(c)
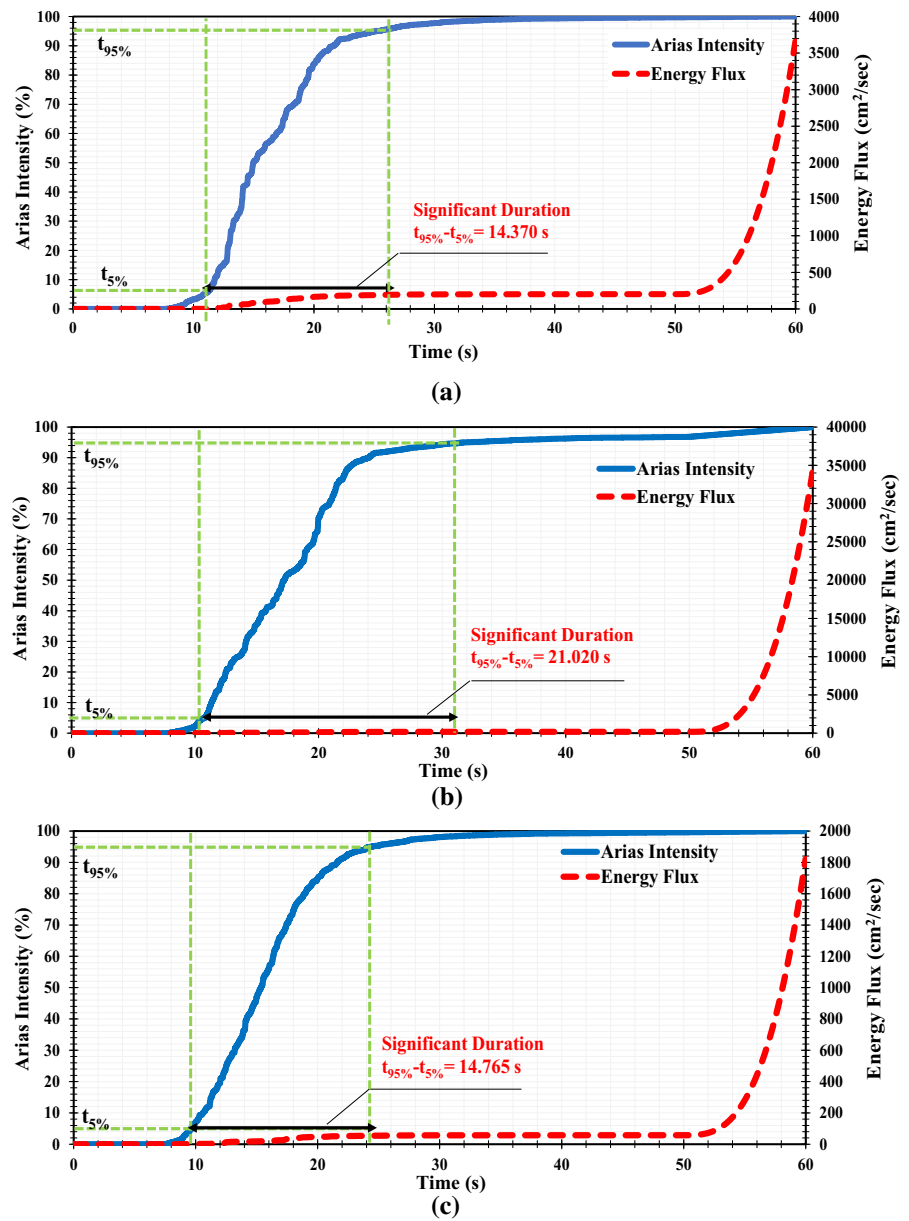
spectral acceleration was recorded at bedrock, since the MSAA is located on a rock site (Mase et al. 2018a). Because this maximum spectral acceleration was at recorded at the bedrock where the MSAA is located, it is expected that the spectral acceleration at ground surface may be even larger due to amplification effects, which would yield even worse damage. Figure 7 also shows that during the resonance period (0.4 to 0.6 s), spectral acceleration ranged from 0.28 to 0.33 g; because this spectral acceleration value range

was recorded during the resonance period, it can be interpreted as the dominant spectral acceleration which buildings were subjected to during the Tarlay Earthquake. It is customary to simplify a building's natural period as $T_n = 0.1n$, where n is the number stories in the building. Therefore, a period of 0.4 to 0.6 s can be described as a natural period for low to medium rise buildings 4 to 6 floors high. Generally, the spectral acceleration of the Tarlay Earthquake was slightly larger in the NS direction than other
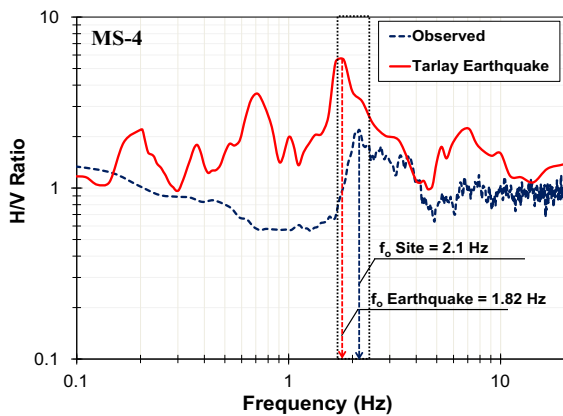
Fig. 6 Comparison of predominant frequency between ground structure and Tarlay Earthquake ground motion
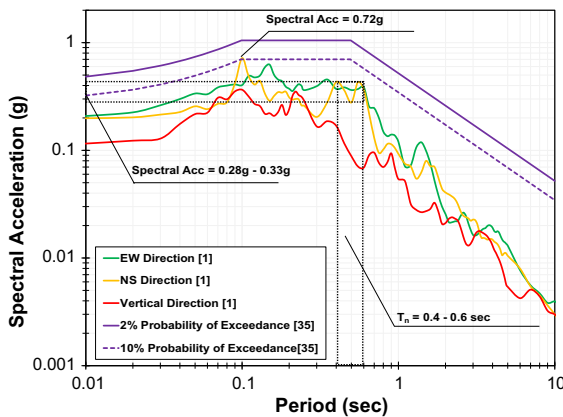

Fig. 7 Comparison of recorded ground motion spectral accelerations during the Tarlay Earthquake to Thai Design Seismic (2009) for earthquake resistance buildings

directions; this finding agrees with Ornthammarath (2013) and Mase et al. (2018b), which stated that the NS directional ground motion of the Tarlay Earthquake recorded at the MSAA most accurately reflected possible earthquake impact due to ground displacement.

4.3 Ground Motion Effect to Liquefaction at Investigated Site

Ground motion interpretations also explained that PGA on each direction has exceeded the threshold of peak ground acceleration to yield liquefaction, i.e. 0.1 g (Kramer 1996). It seems to be the reason why liquefaction could occur in the region, as reported by Mase et al. (2018b, 2020a). Resonance between

ground motion and site could enhance ground motion, particularly once it is approaching ground surface (Paudyal et al. 2012). Yang et al. (2002) mentioned that vertical ground motion could be significantly amplified at ground surface, but horizontal acceleration could not, especially during strong shaking. However, once ground motions on both components take place together (mostly in real cases), the increase of plasticity can happen and it can lead to liquefaction (Tsaparli et al. 2016). It may be caused by the combination between amplification and reduction of effective confining pressure. Horizontal component significantly contribute in pore pressure build-up and vertical component contribute in resulting large acceleration through the layers due to the amplifcation effect.

In line with the observations, it can be observed that ground motions of Tarlay Eartqhuake are relatively large, i.e. 0.2 g. Several studies (Mase et al. 2018b, 2020a, b) considering horizontal component of Tarlay Earthquake ground motion to observe liquefaction potential had confirmed liquefaction in Northern Thailand. Based on the observation, both components show peak values of large horizontal ground motion at base (beyond 0.2 g). It is in line with Yang et al. (2002) who mentioned that horizontal component could significantly induce liquefaction at saturated sandy soils. In the study area, the similar effect of horizontal component could also contribute to trigger pore pressure build-up in saturated sandy soils. The resonance effect also plays important role in yielding liquefaction in the study area. The resonance effect due to vertical ground motion could lead to liquefaction earlier (Tsaparli et al. 2017). Mase et al. (2018b, 2020a, b) showed that liquefaction at the border of Thailand–Myanmar during the Tarlay Earthquake first occurred within first 12 s (the duration of shaking is 60 s) in which peak input motion at the period is about 0.1 g. It means that liquefaction could occur before maximum peak ground acceleration taking place (see Table 1). Therefore, it can be concluded that liquefaction in the region during the Tarlay Earthquake had been induced by the combination effect between both vertical and horizontal ground motions.

5 Conclusion

This study presents the analysis of ground motion parameters and observation of resonance effect during the strong earthquake in Northern Thailand. Several research, such as the dominant ground motion during the earthquake and the tendency of site comparison in identification of resonance are presented. It is identified that during the Tarlay Earthquake of March 2011, the NS component of ground motion recorded at the MSAA is the most impactful direction of ground motion. A large peak amplitude of acceleration, a longer significant duration, and the maximum shaking energy all verify that during the Tarlay Earthquake, the NS component of ground motion played a more significant role than the other directional ground motion components. Results also reveal that soil damage during the Tarlay Earthquake probably more seriously impacted low to medium high-rise buildings. The implementation of H/V ratio is successfully implemented to determine the possibility of resonance effect during the strong earthquake. Resonance effects are suspected to have more contribution to the damage of structural buildings during the Tarlay Earthquake along the Northern Border of Thailand with Myanmar. The results of this study have successfully interpreted the ground motion parameters and the effect of resonance between site and ground motion. Both horizontal and vertical components are predicted to contribute in trigering liquqfeaction in the region. The results of this study would suggest to investigate the study area by performing seismic response analysis due to the NS component of ground motion, specifically and investigate the role of vertical component of ground motion in triggering liquefaction in the study area. In addition, the results also would suggest the local engineers to consider earthquake impact in Northern Thailand. Finally, these results are expected to provide a better understanding of earthquake characteristics in Northern Thailand.

References

Arias A (1970) A measure of earthquake intensity. In: Hansen RJ (ed) Seismic design for nuclear power plants. MIT Press, Cambridge, pp 438–483

Atakan K (2009) The need for standardized approach for estimating the local site effects based on ambient noise recordings. In: Mucciarelli M, Herak M, Cassidy J (eds) Increasing seismic safety by combining engineering technologies and seismological data. NATO science for peace and security series C: environmental security. Springer, Dordrecht, pp 3–15

Bard PY (2004) The SESAME-FP5 Project: an overview and main results. In: Proceeding of the 13th world conference on earthquake engineering, Vancouver, Canada, 1–6 August

Benjamin JR & Associates (1988) A criterion for determining exceedance of the Operating Basis Earthquake, EPRI Report NP-5930. Electric Power Research Institute, Palo Alto, California, USA

Bommer JJ, Martínez-Pereira A (2000) Strong motion parameters: definition, usefulness and predictability. In: Proceedings of the 12th world conference on earthquake engineering, Auckland, 30 January–4 February, New Zealand

Bonnefoy-Claudet S, Cornou C, Bard PY, Cotton F, Moczo P, Kristek J, Fah D (2006) H/V ratio: a tool for site effects evaluation, results from 1-D noise simulations. Geophys J Int 167(2):827–837. https://doi.org/10.1111/j.1365-246x.2006.03154.x

Cabañas L, Benito B, Herráiz M (1997) An approach to the measurement of the potential structural damage of earthquake ground motions. Earthq Eng Struct Dyn 26(1):79–92. https://doi.org/10.1002/(sici)1096-9845(199701)26:1%3c79:aid-eqe624%3e3.0.co;2-y

El-Hady S, Azeem Fergany EA, Othman A, Mohammed A (2012) Seismic microzonation of Marsa Alam, Egypt using inversion HVSR of microtremor observations. J Seismol 16(1):55–66. https://doi.org/10.1007/s10950-011-9249-4

Fischer EG, Fischer TP (1998) Quasi-resonance effects observed in the 1994 Northridge earthquake, and others. Shock Vib 5(3):153–158

Flores J, Novaro O, Seligman TH (1987) Possible resonance effect in the distribution of earthquake damage in Mexico City. Nature 326:783–785. https://doi.org/10.1038/326783a0

Google Earth (2016) Mae Sai-Mae Lao (Northern Thailand Region). http://www.google.com. Accessed 17 Sept 2016

Gosar A (2010) Site effects and soil–structure resonance study in the Kobarid basin (NW Slovenia) using microtremors. Natl Hazards Earth Syst Sci 10(4):761–772. https://doi.org/10.5194/nhess-10-761-2010

Idriss IM, Boulanger RW (2006) Semi-empirical procedures for evaluating liquefaction potential during earthquakes. Soil Dyn Earthq Eng 26(2–4):115–130. https://doi.org/10.1016/j.soildyn.2004.11.023

Kanai K, Tanaka T (1954) Measurement of the microtremor. Bull Earthq Res Inst 32(1):199–209

Koçkar MK, Akgün H (2012) Evaluation of the site effects of the Ankara Basin, Turkey. Appl Geophys 83(1):120–134. https://doi.org/10.1016/j.jappgeo.2012.05.007

Kramer SL (1996) Geotechnical earthquake engineering. Prentice Hall, New Jersey

Lachet C, Bard PY (1994) Numerical and theoretical investigations on the possibilities and limitations of Nakamura's technique. Phys Earth 42(1):377–397. https://doi.org/10.4294/jpe1952.42.377

Lachet C, Hatzfeld D, Bard PY, Theodulidis N, Papaioannon C, Savaidis A (1996) Site effect and microzonation in the City of Thessaloniki (Greece): comparison of different approaches. Bull Seismol Soc Am 86(1):1703–1962

Likitlersuang S, Plengsiri P, Mase LZ, Tanapalungkorn W (2020) Influence of spatial variability of ground on seismic response analysis: a case study of Bangkok subsoils. Bull Eng Geol Environ 79(1):39–51. https://doi.org/10.1007/s10064-019-01560-9

Mase LZ, Tobita T, Likitlersuang S (2017) One-dimensional analysis of liquefaction potential: case study in Chiang Rai Province, Northern Thailand. J Jpn Soc Civ Eng Ser A1 (Struct Eng/Earthq Eng) 73(4):I_135–I_147. https://doi.org/10.2208/jscejseee.73.i_135

Mase LZ, Likitlersuang S, Tobita T (2018a) Analysis of seismic ground response caused during strong earthquake in Northern Thailand. Soil Dyn Earthq Eng 114(11):113–126. https://doi.org/10.1016/j.soildyn.2018.07.006

Mase LZ, Likitlersuang S, Tobita T (2018b) Non-linear site response analysis of soil sites in Northern Thailand during the M_w 6.8 Tarlay Earthquake. Eng J 22(3):291–303. https://doi.org/10.4186/ej.2018.22.3.291

Mase LZ, Likitlersuang S, Tobita T (2020a) Verification of liquefaction potential during the strong earthquake at the border of Thailand–Myanmar. J Earthq Eng. https://doi.org/10.1080/13632469.2020.1751346

Mase LZ, Likitlersuang S, Tobita T, Chaiprakaikeow S, Soralump S (2020b) Local site investigation of liquefied soils caused by earthquake in Northern Thailand. J Earthq Eng 24(7):1181–1204. https://doi.org/10.1080/13632469.2018.1469441

Misliniyati R, Mase LZ, Irsyam M, Hendriawan H, Sahadewa A (2019) Seismic response validation of simulated soil models to vertical array record during a strong earthquake. J Eng Technol Sci 51(6):772–790

Nakamura Y (1989) A method for dynamic characteristic estimation of subsurface using microtremor on ground surface. Q Rep Railway Tech Res 30(1):25–53

National Earthquake Hazards Reduction Program (NEHRP) (1998) FEMA 302: recommended provisions for seismic regulation for new buildings and other structures (1997) Edition Part 1-provisions and part 2-commentary, FEMA, USA

Nuttli OW (1979) The relation of sustained maximum ground acceleration and velocity to earthquake intensity and magnitude, Miscellaneous Paper S-71-1, Report 16, U.S. Army Corps of Engineers, Waterways Experiment Station, Vicksburg, Mississippi, USA

Ornthammarath T (2013) A note on the strong ground motion recorded during the M_w 6.8 earthquake in Myanmar on 24

March 2011. Bull Earthq Eng 11(1):241–254. https://doi.org/10.1007/s10518-012-9385-4

Park YJ, Ang AHS, Wen YK (1985) Seismic damage analysis of reinforced concrete buildings. J Struct Eng 111(4):740–757. https://doi.org/10.1061/(asce)0733-9445(1985)111:4(740)

Paudyal YR, Yatabe R, Bhandary NP, Dahal RK (2012) A study of local amplification effect of soil layers on ground motion in the Kathmandu Valley using microtremor analysis. Earthq Eng Eng Vib 11(2):257–268. https://doi.org/10.1007/s11803-012-0115-3

Phodee P, Trisirisatayawong I, Aobpaet A (2015) Coseismic and postseismic displacement of 2011 Mw 6.8 Tarlay Earthquake, Myanmar using InSAR techniques and inversion analysis. Eng J 19(2):157–169. https://doi.org/10.4186/ej.2015.19.2.157

Raptakis DG, Manakou MV, Chavez-Garcia FJ, Makra KA, Pitilakis KD (2005) 3D Configuration of Mygdonian Basin and Preliminary estimate of its site response. Soil Dyn Earthq Eng 25(1):871–887. https://doi.org/10.1016/j.soildyn.2005.05.005

Rathje EM, Abrahamson NA, Bray JD (1998) Simplified frequency content estimates of earthquake ground motions. J Geotech Geoenviron Eng (ASCE) 124(2):150–159. https://doi.org/10.1061/(asce)1090-0241(1998)124:2(150)

Ruangrassamee A, Ornthammarath T, Lukkunaprasit P (2012) Damage due to 24 March 2011 M6.8 Tarlay earthquake in Northern Thailand. In: Proceeding the 15th world conference on earthquake engineering, Lisboa, 24–28 September

Sarma SK, Yang KS (1987) An evaluation of strong motion records and a new parameter A95. Earthq Eng Struct Dyn 15(1):119–132. https://doi.org/10.1002/eqe.4290150109

Seed HB, Idriss IM (1971) Simplified procedure for evaluating soil liquefaction potential. J Soil Mech Found Div ASCE 97(6):1249–1273

Seismosoft (2018) SeismoSignal Program, Seismosoft. http://www.seismosoft.com

Senna S, Fujiwara H (2008) Development of analyzing tools for microtremor survey observation data, Technical Note of the National Research Institute for Earth Science and Disaster Prevention 1(313)

Soralump S, Feungaugsorn J (2013) Probabilistic analysis of liquefaction potential: the first eyewitness case in Thailand. In: Proceeding of the 18th national convention of civil engineering, Chiang Mai, Thailand, 8–10 May

Tanapalungkorn W, Mase LZ, Latcharote P, Likitlersuang S (2020) Verification of attenuation models based on strong ground motion data in Northern Thailand. Soil Dyn Earthq Eng 133(106145):1–9. https://doi.org/10.1016/j.soildyn.2020.106145

Thai Department of Mineral Resources (TDMR) (2017) Mae Sai geological map. Thailand Department of Mineral Resources, Bangkok

Thai Design Seismic (TDS) (2009) Seismic Design Code of Thailand. Department of Public Works and Town-Country Planning, Ministry of Interior, Bangkok, Thailand

Thai Meteorological Department (TMD) (2011) Earthquake Data of Thailand in 2011. Thailand Meteorological Department, Bangkok, Thailand

Thay S, Likitlersuang S, Pipatpongsa T (2013) Monotonic and cyclic behavior of Chiang Mai sand under simple shear

mode. Geotech Geol Eng 31(1):67–82. https://doi.org/10.1007/s10706-012-9563-9

Tsaparli V, Kontoe S, Taborda DMG, Potts DM (2016) Vertical ground motion and its effects on liquefaction resistance of fully saturated sand deposits. Proc R Soc A 472(20160434):1–21. https://doi.org/10.1098/rspa.2016.0434

Tsaparli V, Kontoe S, Taborda DM, Potts DM (2017) An energy-based interpretation of sand liquefaction due to vertical ground motion. Comput Geotech 90:1–13. https://doi.org/10.1016/j.compgeo.2017.05.006

Von Thun JL, Rochim LH, Scott GA, Wilson JA (1988) Earthquake ground motions for design and analysis of dams. In: Von Thun JL (eds) Earthquake engineering and soil dynamics II—recent advances in ground-motion evaluation. Geotechnical Special Publication, pp 463–481

Yang J, Sato T, Savidis S, Li XS (2002) Horizontal and vertical components of earthquake ground motions at liquefiable sites. Soil Dyn Earthq Eng 22(3):229–240. https://doi.org/10.1016/s0267-7261(02)00010-6

Youd TL, Idriss IM (2001) Liquefaction resistance of soils: summary report from the 1996 NCEER and 1998 NCEER/NSF workshops on evaluation of liquefaction resistance of soils. J Geotech Geoenviron Eng ASCE 127(4):297–313. https://doi.org/10.1061/(asce)1090-0241(2001)127:10(817)